TRANSIENT CONDUCTION-RADIATION HEAT TRANSFER IN MULTI-LAYER PLANAR PARTICIPATING MEDIA WITH FLUX BOUNDARY CONDITION

Gino Genaro and **Orosimbo Andrade de Almeida Rego**
Federal University of Uberlândia - Mechanical Engineering Department
Rua Salvador Lahoz, 413. Ap. 34.
12238-220 São José dos Campos-SP, Brazil
E-mail: ggenaro@dem.inpe.br, oaarego@ufu.br

José Bezerra Pessoa Filho
Aerospace Technical Center - Institute of Aeronautics and Space
12228-904 São José dos Campos-SP, Brazil
E-mail: jbp@iae.cta.br

Abstract. Transient and steady state combined conduction-radiation heat transfer between parallel flat plates separated by semitransparent media is investigated. The boundaries are assumed to be opaque and gray. The medium separating the plates emits, absorbs and isotropically scatters thermal radiation. A prescribed heat flux is applied at one of the boundaries. Based upon the application of the overall energy and radiative conservation principles, a relationship between the two heat transfer modes, i.e., radiation and conduction, is established. The space and time derivatives are discretized according to the finite difference method. To solve the Radiative Transfer Equation - RTE, a novel discretization scheme is used. Effects of conduction-radiation parameter, optical thickness and surface emissivities on the temperature and heat flux distribution are analyzed within the medium. The obtained results are compared against others available in the literature.

Key words: *thermal radiation, radiative transfer equation (RTE), transient conduction-radiation heat transfer*

1. Introduction

The several practical applications in which energy transfer is due to coupled conduction and radiation have motivated, during the last three decades, the study of such a problem. Most of the investigations are concerned with the steady state heat exchange between two infinite plane parallel surfaces, kept at constant known temperatures, separated by one or more layers of semitransparent materials (Viskanta, 1964; Tarshis et al., 1969; Yuen and Wong, 1980; Ho and Özisik, 1986; Genaro et al., 2001). The transient analysis is more involved. In this case, the temperature distribution within semitransparent media can be strongly affected by internal emission, absorption and scattering of radiant thermal energy. In many practical applications it is necessary to know, with good precision, the behavior of temperature distribution within the medium during transient state. These are the case, for example, of glass thermal treatment process, design of ablative thermal protection systems and thermal control of rocket's motors. The literature presents several investigations related to this subject, much of them regarding with infinite plane parallel plates, kept at constant temperatures and separated by semitransparent medium (Doornink and Hering, 1972; Weston and Hauth, 1973; Genaro et al., 2002). There are more complex situations, where temperatures at the boundaries are unknown and the boundary conditions are of prescribed flux type (Ho and Özisik, 1987; Glass et al., 1987). A comprehensive overview on the transient effects of radiative transfer in semitransparent materials is given by Siegel (1998).

This work considers transient combined conduction-radiation heat transfer between two infinite plane parallel surfaces, separated by a semitransparent medium composed by one or more layers with prescribed heat flux as boundary condition. Later on, the equations describing the phenomena and the method of solution are presented and the obtained results compared with values published by other authors.

2. Formulation

The geometrical configuration studied in this work is shown in Fig. (1). The medium is composed by N layers of semitransparent materials that absorb, emit and isotropically scatter radiation. The interfaces separating two different layers are assumed to be transparent. The optical properties of the materials can change from one layer to another, but are constant and uniform within each layer. The boundary surfaces are gray, diffuse and opaque, with emissivities, ε. The medium is initially at zero temperature. For times greater than zero, a constant radiation heat flux Q_0 is applied on the boundary surface located at $\tau = 0$. Heat is dissipated externally by radiation from both surfaces, located at $\tau = 0$ and $\tau = \tau_0$, into an ambient at zero temperature.

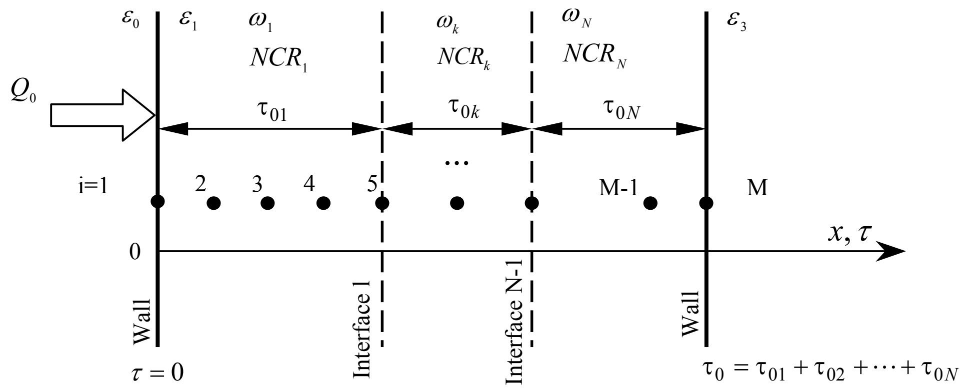

Figure 1. Geometrical configuration.

The application of the overall energy conservation principle to an infinitesimal volume element within the medium, under the assumption of one-dimensional transient heat transfer and constant physical properties, yields (Özisik, 1973)

$$\frac{\partial \theta(\tau,\xi)}{\partial \xi} = \frac{\partial^2 \theta(\tau,\xi)}{\partial \tau^2} - \frac{1}{4NCR_k}\frac{\partial Q^r(\tau,\xi)}{\partial \tau}, \qquad 0 < \tau < \tau_o, \ \xi > 0 \text{ and } k = 1,\cdots,N \tag{1.a}$$

with the boundary conditions

$$Q_{abs} - \varepsilon_0 \theta^4(0,\xi) - Q^r(0,\xi) + 4NCR_1 \frac{\partial \theta(0,\xi)}{\partial \tau} = 0, \qquad \tau = 0 \text{ and } \xi > 0 \tag{1.b}$$

$$-4NCR_N \frac{\partial \theta(\tau_0,\xi)}{\partial \tau} + Q^r(\tau_0,\xi) - \varepsilon_3 \theta^4(\tau_0,\xi) = 0, \qquad \tau = \tau_0 \text{ and } \xi > 0 \tag{1.c}$$

$$NCR_k \left.\frac{d\theta(\tau,\xi)}{d\tau}\right|_{Interface\,l} = NCR_{k+1} \left.\frac{d\theta(\tau,\xi)}{d\tau}\right|_{Interface\,l} \quad \text{at the interfaces, } l = 1,\cdots,N-1 \text{ and } \xi > 0 \tag{1.d}$$

and initial condition

$$\theta(\tau,0) = 0, \text{ for } 0 \le \tau \le \tau_0 \text{ and } \xi = 0. \tag{1.e}$$

where Q_{abs}, θ, ξ, τ and NCR_k refer to dimensionless absorbed heat flux, temperature, time, optical thickness variable and conduction-radiation parameter of layer k defined, respectively, by

$$Q_{abs} = \varepsilon_0 Q_0, \quad \theta(\tau,\xi) \equiv \frac{T(x,t)}{T_r}, \quad \xi \equiv \alpha_k \beta_k^2 t, \quad \tau \equiv \beta_k x \quad \text{and} \quad NCR_k \equiv \frac{k_k \beta_k}{4r^2 \sigma T_r^3} \tag{2.a,b,c,d,e}$$

where the subscript "k" denotes the different materials which the medium is made of. The parameters α_k, β_k, τ_{0k}, k_k, x, t, T and r are the thermal diffusivity, extinction coefficient, total optical thickness and thermal conductivity of layer k, physical length variable, time, temperature and refraction index, respectively; σ is the Stefan-Boltzmann constant and T_r is a reference temperature. τ_0 is the total optical thickness, including all layers of the medium. A more detailed explanation about the radiative parameters can be obtained in Modest (1993).

The last term in Eq. (1.a) refers to the divergence of the dimensionless radiative heat flux, given by (Özisik, 1973)

$$\frac{\partial Q^r(\tau,\xi)}{\partial \tau} = 4(1-\omega_k)\left[\theta^4(\tau,\xi) - G^*(\tau,\xi)\right], \quad \text{with} \quad k = 1,\cdots,N \tag{3}$$

where ω_k is the scattering albedo of layer k and $G^*(\tau,\xi)$ and $Q^r(\tau,\xi)$ are the dimensionless incident radiation and net radiative heat flux defined by

$$G^*(\tau,\xi)=\frac{G(\tau,\xi)}{4r^2\sigma T_r^4} \quad \text{and} \quad Q^r(\tau,\xi)=\frac{q^r(\tau,\xi)}{r^2\sigma T_r^4}. \tag{4.a,b}$$

The quantities $G(\tau,\xi)$ and $q^r(\tau,\xi)$ appearing in Eqs. (4.a,b) are defined, respectively, as

$$G(\tau,\xi)=2\pi\int_{-1}^{1} I(\tau,\mu,\xi)\,d\mu \quad \text{and} \quad q^r(\tau,\xi)=2\pi\int_{-1}^{1} I(\tau,\mu,\xi)\,\mu d\mu, \tag{5.a,b}$$

where $I(\tau,\mu,\xi)$ is the intensity of radiation at a position τ, time ξ and direction θ $(\mu=\cos\theta)$, Fig. (2).

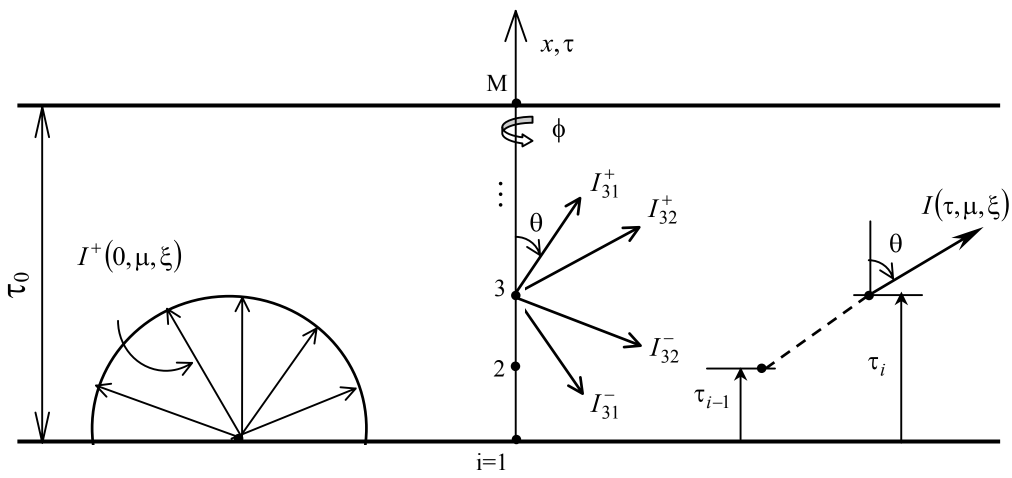

Figure 2. Schematic diagram of physical model, coordinates and discretization of I(τ,μ,ξ).

$I(\tau,\mu,\xi)$ is obtained by applying the conservation of radiative energy principle to an infinitesimal volume element inside the medium obtaining the so-called Radiative Transfer Equation (RTE), Özisik (1973):

$$\mu\frac{dI(\tau,\mu,\xi)}{d\tau}+I(\tau,\mu,\xi)=S(\tau,\xi), \tag{6.a}$$

where $S(\tau,\xi)$ is the source term given by

$$S(\tau,\xi)=[1-\omega_k]I_b[\theta(\tau,\xi)]+\frac{\omega_k}{2}\int_{-1}^{1} I(\tau,\mu,\xi)\,d\mu, \quad \text{with} \quad k=1,\cdots,N. \tag{6.b}$$

In obtaining Eqs. (6.a,b), we assumed a gray, isotropically scattering medium with constant optical properties. It has also been assumed that the intensity of radiation is independent on the azimuth angle ϕ. Equations (6.a,b) are valid for any layer within the medium and are evaluated at each time ξ. $I_b[\theta(\tau,\xi)]$ is the Planck function, which depends on the medium's temperature, and it is given by

$$I_b[\theta(\tau,\xi)]=\frac{r^2\,\sigma\theta^4(\tau,\xi)}{\pi T_r^4}. \tag{7}$$

At the walls,

$$I^+(0,\mu,\xi)=\varepsilon_1 I_b(\theta_1)+2(1-\varepsilon_1)\int_0^1 I^-(0,-\mu',\xi)\mu' d\mu', \quad 0<\mu\le 1 \tag{8.a}$$

$$I^-(\tau_o,-\mu,\xi)=\varepsilon_2 I_b(\theta_2)+2(1-\varepsilon_2)\int_0^1 I^+(\tau_o,\mu',\xi)\mu' d\mu', \quad 0<\mu\le 1 \tag{8.b}$$

where $I^+(\tau,\mu,\xi)$ and $I^-(\tau,-\mu,\xi)$ are, respectively, the forward and backward radiation intensities.

The objective of solving Eqs. (1)-(8) is to find the temperature distribution within the medium and investigate how it is affected by the physical and optical properties of the medium, as well as by its boundary conditions. By solving Eqs. (1), it is possible to obtain the temperature distribution within the medium. However, solution of Eqs. (1) requires the knowledge of the divergence of $Q^r(\tau,\xi)$, which depends on $G^*(\tau,\xi)$, as shown by Eq. (3). To obtain $G(\tau,\xi)$, it is necessary to solve the RTE which, by its turn, depends on the temperature distribution within the medium. Therefore, we have a coupled radiative-conductive heat transfer problem whose solution is of iterative type.

3. Solution method

The solution method consists of solving simultaneously the overall energy equation and the radiative transfer equation, Eqs. (1) and (6), respectively. For the sake of clarity, the presentation of the method is divided into three steps.

3.1. Conduction problem

Equation (1.a) is discretized according to a second order central difference scheme for the space variable and a fully implicit finite difference scheme in time. As a consequence, Eq. (1.a) becomes

$$\frac{(\theta_{i-1})^{(n+1)}}{BCK(i)}-\left[\frac{1}{\Delta\xi}+\frac{1}{FWD(i)}+\frac{1}{BCK(i)}+\frac{4(1-\omega_k)}{NCR_k}\left(\theta_i^3\right)^{(n)}\right](\theta_i)^{(n+1)}+\frac{(\theta_{i+1})^{(n+1)}}{FWD(i)}=$$
$$=-\left[\frac{(\theta_i)^{(n)}}{\Delta\xi}+\frac{1-\omega_k}{NCR_k}\left(3\left(\theta_i^4\right)^{(n)}-G_i^*\right)\right] \tag{9.a}$$

where i refers to the grid points located within the medium, Fig. (1). The superscript n refers to the previous time step, whereas $n+1$ refers to the time step whose solution is being sought. Therefore, $n=0$ corresponds to the initial condition at $\xi=0$.

At the boundaries and the interfaces Eqs. (1.b,c,d) are discretized utilizing a first order scheme for the space variable. The heat capacity is not neglected in view of the high radiation flux level applied at $\tau=0$. Therefore, a fully implicit finite difference scheme is utilized for the time variable, yielding

$$\left[\frac{2NCR_k\Delta\tau}{\Delta\xi}+4\varepsilon_0\theta_1^{3^{(n)}}+\frac{4NCR_k}{\Delta\tau}\right]\theta_1^{(n+1)}+\left[-\frac{4NCR_k}{\Delta\tau}\right]\theta_2^{(n+1)}=$$
$$=Q_{abs}+3\varepsilon_0\theta_1^{4^{(n)}}-\frac{Q_1^{r^{(n)}}+Q_2^{r^{(n)}}}{2}+\frac{2NCR_k\Delta\tau}{\Delta\xi}\theta_1^{(n)} \qquad \text{for } \tau=0 \text{ and } \xi>0 \tag{9.b}$$

$$\left[\frac{4NCR_k}{\Delta\tau}\right]\theta_{M-1}^{(n+1)}-\left[\frac{4NCR_k}{\Delta\tau}+4\varepsilon_3\theta_M^{3^{(n)}}+\frac{2NCR_k\Delta\tau}{\Delta\xi}\right]\theta_M^{(n+1)}=$$
$$=-\frac{2NCR_k\Delta\tau}{\Delta\xi}\theta_M^{(n)}-\frac{Q_{M-1}^{r^{(n)}}+Q_M^{r^{(n)}}}{2}-3\varepsilon_3\theta_M^{4^{(n)}} \qquad \text{for } \tau=\tau_0 \text{ and } \xi>0 \text{ and} \tag{9.c}$$

$$\left(\frac{-NCR_k}{\tau_i-\tau_{i-1}}\right)\theta_{i-1}^{n+1}+\left(\frac{NCR_k}{\tau_i-\tau_{i-1}}+\frac{NCR_{k+1}}{\tau_{i+1}-\tau_i}\right)\theta_i^{n+1}+\left(\frac{-NCR_k}{\tau_{i+1}-\tau_i}\right)\theta_{i+1}^{n+1}=0 \qquad \text{at the interfaces,} \tag{9.d}$$

where FWD(i) and BCK(i) are given by

$$FWD(i)=(\tau_{i+1}-\tau_i)\left(\frac{\tau_{i+1}-\tau_{i-1}}{2}\right) \quad \text{and} \quad BCK(i)=(\tau_i-\tau_{i-1})\left(\frac{\tau_{i+1}-\tau_{i-1}}{2}\right). \tag{10.a,b}$$

In order to avoid numerical problems, the fourth power terms $\theta^4(\tau,\xi)$ present in Eqs. (1.b,c) and Eq.(3) are linearized according to $\theta_i^{4^{(n+1)}}=4\theta_i^{3^{(n)}}\theta_i^{(n+1)}-3\theta_i^{4^{(n)}}$. To cluster more nodes near the boundaries and the interfaces, where large temperature gradients are expected, a variable grid size given by $\tau_{i+1}=\tau_i+f_r\times(\tau_i-\tau_{i-1})$, $i=2,3,\cdots,M-1$, is used. As initial values of the grid size, it was taken $\tau_1=0$ and $\tau_2=\Delta\tau$, with f_r, the stretching factor of the mesh. Since large temperature variations are also expected at the beginning of the transient process, a variable time step given by $\Delta\xi^n = 1 - e^{-\gamma n}$, is used. Here, γ defines the rate of increase of $\Delta\xi$, and n is the time step counter $(n = 0,1,2,3,\cdots)$.

The radiative heat flux term on the right-hand side of Eqs. (9.b,c) is taken as an average value between nodes located at the boundaries, i.e., between nodes 1 and 2, at $\tau = 0$, and between M-1 and M, at $\tau = \tau_0$. Solution of Eqs. (9) gives the temperature profile within the medium at time step $n+1$. Nonetheless, they can only be solved if $Q^r(\tau,\xi)$ and $G^*(\tau,\xi)$ are known. To obtain them, the RTE solution is required.

3.2. Radiation problem

To solve the RTE we integrate Eqs. (6.a,b), between τ_{i-1} and τ_i, along a given μ-direction within the medium, Fig. (2), obtaining

$$I(\tau_i,\mu,\xi) = I(\tau_{i-1},\mu,\xi)\,e^{-(\tau_i - \tau_{i-1})/\mu} + \bar{S}(\tau,\xi)\left[1 - e^{-(\tau_i - \tau_{i-1})/\mu}\right], \quad -1 \le \mu < 0 \text{ and } 0 < \mu \le 1 \tag{11}$$

where $\bar{S}(\tau,\xi)$ represents the average value of $S(\tau,\xi)$, Eq. (6.b), between τ_{i-1} and τ_i. In obtaining Eq. (11), isotropic scattering and a constant value of β_k are assumed. For the sake of simplicity, we define

$$I^-(\tau,\mu,\xi) = I(\tau,\mu,\xi), \quad -1 \le \mu < 0 \quad \text{and} \quad I^+(\tau,\mu,\xi) = I(\tau,\mu,\xi), \quad 0 < \mu \le 1. \tag{12.a, b}$$

Due to the discontinuity of $I(\tau,\mu,\xi)$ at $\mu = 0$ ($\theta = 90^o$), the interval $-1 \le \mu \le 1$ is divided into two parts, prior to the application of the numerical integration method (Pessoa-Filho and Thynell, 1994), and Eqs. (5.a,b) become

$$G(\tau,\xi) = 2\pi\int_{-1}^{1} I(\tau,\mu,\xi)d\mu = 2\pi\left(\int_{-1}^{0} I^-(\tau,\mu,\xi)d\mu + \int_{0}^{1} I^+(\tau,\mu,\xi)d\mu\right), \tag{13.a}$$

$$q^r(\tau,\xi) = 2\pi\int_{-1}^{1} I(\tau,\mu,\xi)\mu d\mu = 2\pi\left(\int_{-1}^{0} I^-(\tau,\mu,\xi)\mu d\mu + \int_{0}^{1} I^+(\tau,\mu,\xi)\mu d\mu\right). \tag{13.b}$$

Since the discontinuity of the integrand has been considered, a quadrature formulae is now applied to numerically evaluate the integrals appearing on the right-hand side of Eqs. (13.a,b). The application of a Gaussian quadrature formulae to Eqs. (13.a,b), yields

$$G(\tau,\xi) \approx G_i = \pi\sum_{j=1}^{N_q} \varsigma_j\left(I_{ij}^- + I_{ij}^+\right), \quad q^r(\tau,\xi) \approx q_i^r = q_i^+ + q_i^-, \quad \text{with} \quad q_i^\pm = \pi\sum_{j=1}^{N_q}\varsigma_j \mu_j^\pm I_{ij}^\pm, \tag{14.a,b,c}$$

where ς_j are the weights given by the quadrature formulae and N_q is the number of quadrature points. In writing Eqs. (14.a,c), the notation $I_{ij}^\pm = I(\tau_i,\mu_j^\pm)$ is used, where the subscripts i and j refer to the τ- and μ-direction, respectively. It should be mentioned that N_q gives half of the number of angular directions in which $I(\tau,\mu,\xi)$ is discretized. Therefore, $N_q = 2$ indicates that $I(\tau,\mu,\xi)$ is evaluated along four directions, namely, two in the positive-direction, $0 < \mu \le 1$, and two in the negative-direction, $-1 \le \mu < 0$, as schematically shown in Fig. 2. Since the zeroes of the Gaussian quadrature formulae are defined for a continuous integration interval [-1,1], they need to be shifted to the intervals [-1,0] and [0,1], according to the equation

$$\mu_j^\pm = 0.5\left[\zeta_j \pm 1\right] \qquad j = 1,2,\cdots,N_q, \tag{15}$$

where ζ_j are the zeroes of the Gaussian quadrature formulae as defined to the interval [-1,1]. Equation (11) can now be written as

$$I_{ij}^+ = I_{i-1,j}^+\; e^{-(\tau_i - \tau_{i-1})/\mu_j} + \bar{S}_{ij}^+\left[1 - e^{-(\tau_i - \tau_{i-1})/\mu_j}\right], \qquad i = 2,\cdots,M, \tag{16.a}$$

$$I_{ij}^- = I_{i+1,j}^- \; e^{-(\tau_{i+1}-\tau_i)/\mu_j} + \bar{S}_{ij}^- \left[1 - e^{-(\tau_{i+1}-\tau_i)/\mu_j} \right], \qquad i = 1, \cdots, M-1 . \tag{16.b}$$

where $j = 1, \cdots, N_q$. The approximation of the source function is

$$\bar{S}_{ij}^{\pm} = \left(S_{i\mp1,j} + S_{ij} \right) / 2 , \qquad i = 2, \cdots, M \;\text{ and }\; j = 1, \cdots, N_q . \tag{17}$$

It is worth mentioning that even if the temperature profile in the medium is known, the RTE solution is an iterative one.

The solution procedure to solve the RTE and to obtain $G(\tau, \xi)$ can be summarized as follows:

i) A "guessed" temperature distribution within the medium is assumed (e.g., the initial condition);

ii) $I_{ij}^+ = 0$, $i = 2,3, \cdots, M$, $j = 1,2, \cdots, N_q$

$I_{ij}^- = 0$, $i = 1,2, \cdots, M-1$, $j = 1,2, \cdots, N_q$

$\tilde{G}_i^{old} = G_i^{new} = 0, \; i = 1, \cdots, M$

iii) $I_{1j}^+ = \varepsilon_1 I_b(\theta_1) + 2(1-\varepsilon_1)\left| q_1^- \right|$; $I_{Mj}^- = \varepsilon_2 I_b(\theta_M) + 2(1-\varepsilon_2) q_M^+$; $\qquad j = 1,2, \cdots, N_q$;

iv) Based on steps i), ii) and iii), evaluate G_1^{new} and G_M^{new}, according to

$$G_i^{new} = \pi \sum_{j=1}^{N_q} \varsigma_j \left(I_{ij}^- + I_{ij}^+ \right), \quad i = 1 \text{ and } M$$

v) Evaluate S_1, S_M and $\bar{S}_{ij}^{\pm}$, as follows

$$S_1 = (1-\omega_k) I_b[\theta(\tau_1, \xi)] + \frac{\omega_k}{4\pi} G_1^{new} \;\text{ and }\; S_M = (1-\omega_k) I_b[\theta(\tau_M, \xi)] + \frac{\omega_k}{4\pi} G_M^{new}$$

$$\bar{S}_{ij}^{\pm} = \left(S_{i\mp1,j} + S_{ij} \right) / 2 , \qquad i = 2, \cdots, M \;\text{ and }\; j = 1, \cdots, N_q$$

vi) $I_{ij}^+ = I_{i-1,j}^+ \; e^{-(\tau_i - \tau_{i-1})/\mu_j} + \bar{S}_{ij}^+ \left[1 - e^{-(\tau_i - \tau_{i-1})/\mu_j} \right], \qquad i = 2, \cdots, M$ and $j = 1, \cdots, N_q$

$I_{ij}^- = I_{i+1,j}^- \; e^{-(\tau_{i+1}-\tau_i)/\mu_j} + \bar{S}_{ij}^- \left[1 - e^{-(\tau_{i+1}-\tau_i)/\mu_j} \right], \qquad i = 1, \cdots, M-1$ and $j = 1, \cdots, N_q$

vii) By using Eqs. (14.a,b), G_i^{new} and $q_i^{\pm}$, $i = 1, \cdots, M$, are evaluated;

viii) G_i^{new} and $\tilde{G}_i^{old}$ are compared. If the difference between them is greater than a given tolerance, an under-relaxation scheme is applied on G_i^{new} to speed convergence at each time step, i.e., $\tilde{G}_i^{new} = \tilde{G}_i^{old} + \alpha' \left(G_i^{new} - \tilde{G}_i^{old} \right)$, where α' is the relaxation factor, taken as 0.30, $\tilde{G}_i^{new}$ is the relaxed incident radiation to be used in the next iterative step, $\tilde{G}_i^{old}$ is the relaxed incident radiation obtained in the prior iterative step and G_i^{new} is the incident radiation obtained in step *vii)*.

ix) If $\varepsilon_1 = \varepsilon_2 = 1$, steps iv) through viii) are repeated until the following convergence criterion is verified

$$\sum_{i=1}^{M} \frac{\left| G_i^{new} - \tilde{G}_i^{old} \right|}{G_i^{new}} \leq 10^{-5} \quad . \tag{18}$$

ix) If $\varepsilon_1 \neq 1$ or $\varepsilon_2 \neq 1$, steps iii) through viii) are repeated and the same convergence criterion is used.

3.3. Conduction-radiation problem

In section 3.1 it was described the solution procedure for the conduction part of the problem, assuming that the radiative part was known, i.e., $G^*(\tau, \xi)$ and $Q^r(\tau, \xi)$. To solve the RTE, section 3.2, the temperature within the medium was assumed to be known. Nonetheless, the radiation and conduction problems are coupled and need to be solved simultaneously, requiring an interative type of solution involving Eqs. (9), (14) and (16). It can be summarized as follows:

i) A temperature distribution defined by the initial condition is assumed ($n = 0$);

ii) The temperature distribution for the first time step ($n = 1$) is calculated by solving Eqs. (9). For this calculation, the radiative effects are nulls, because $G_i^* = Q_i^r = 0$, $i = 1,2, \ldots, M$.

iii) Based on the temperature distribution obtained in step ii), the RTE is solved and G_i^* and Q_i^r are calculated.

iv) Based on the temperature distribution for the last time step (n) and on the new values of G_i^* and Q_i^r , Eqs. (9) are solved again, obtaining a new temperature distribution for ($n=1$).
v) The results obtained in steps ii) and iv) are compared. If the difference between them is greater than a given tolerance, an under-relaxation scheme is applied on the temperature to speed convergence at each time step, i.e., $\tilde{\theta}^{new} = \tilde{\theta}^{old} + \alpha'\left(\theta^{new} - \tilde{\theta}^{old}\right)$, where α' is the relaxation factor, taken as 0.30, $\tilde{\theta}^{new}$ is the relaxed temperature to be used in the next iterative step, $\tilde{\theta}^{old}$ is the relaxed temperature obtained in the prior iterative step and θ^{new} is the temperature obtained in step iv). The steps iii) through v) are repeated until the following convergence criteria is reached

$$\sum_{i=1}^{M} \frac{\left|\tilde{\theta}_i^{old} - \theta_i^{new}\right|}{\theta_i^{new}} \leq 10^{-5} \quad . \tag{19}$$

vi) It should be noted that this iterative scheme is applied within the same time step ($n+1$). Only after the convergence criteria is reached the calculations for the next time step will take place. The procedure is conducted until a desired observation time ξ_d is reached.

4. Results and Discussion

In order to validate the proposed method of solution, some simulations are presented. We consider systems formed by one and two layers of semitransparent materials and present temperature distributions within such media as function of optical thickness, conduction-radiation parameter and emissivities of the bounding surfaces. Both transient and steady state conditions are considered. In all simulations, $M=69$, $N_q=2$, $f_r=1.05$, $\gamma = 2.23\times10^{-5}$ and the refractive index, r, is taken equal to unity.

Figure (3) shows the effects of the conduction-radiation parameter, NCR, and optical thickness, τ_0, for a single layer nonscattering medium. The wall at $\tau=0$, has an external emissivity, ε_0, of 0.2, whereas all remaining surfaces are black. Two different values of NCR are investigated, i.e., NCR=0.25 and NCR=5.0. The optical thickness simulated are equal to 1.0 and 10.0. For the sake of comparison, numerical results obtained by Ho and Özisik (1987) are also shown in the figure. These authors have utilized another approximation scheme to solve the radiative transfer equation, based on the generalization of Galerkin method. For $\tau_0=1$, it is observed that the larger NCR the larger is the time to reach steady state. To explain such a behavior, we need to look at the physics of the problem, as well its initial and boundary conditions. The medium is initially at zero temperature and, at $\xi=0$, has transfered to it a given amount of energy, Q_{abs} . This energy is transfered to the inner regions of the medium by two ways: conduction and radiation. The NCR parameter measures the relative importance of each heat transfer mechanism on the energy transfer within the medium. The larger the NCR the more important is conduction heat transfer, as compared to radiation. Going back to the presented results for $\tau_0=1.0$, it is observed that the smaller the NCR the faster is the steady state reached because the energy is more rapidly transfered, by radiation, to the inner regions of the medium. The same behavior is observed for $\tau_0=10.0$.

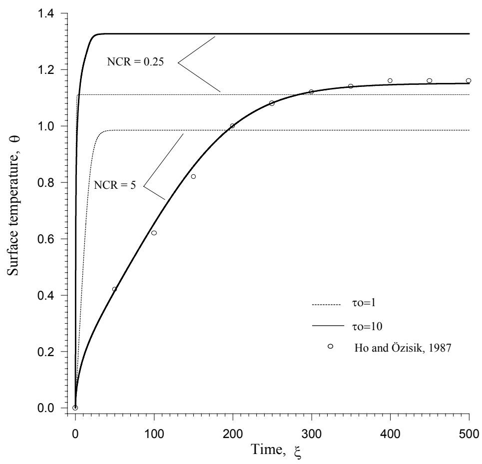

Figure 3. Effects of conduction-radiation parameter and optical thickness on the transient temperature at $\tau=0$ for $\varepsilon_0=0.2$ and $\varepsilon_1=\varepsilon_2=\varepsilon_3=1.0$.

We now turn our attention to the effects of the optical thickness of the medium. For a fixed value of NCR, it is observed that the larger the τ_0 the higher is the final temperature. Such a behavior is also explained by the physics of the problem. A large τ_0 means a more participating medium, i.e., a medium which will absorb more of the radiation passing through it. From the energy conservation principle, the larger the energy absorption by the medium the higher its temperature. For $\tau_0 = 1.0$, the steady state condition is rapidly reached, whereas for $\tau_0 = 10.0$, it takes a while until the temperature at $\tau = 0$ reaches its steady state condition. Since NCR is the same for both cases, τ_0 gives how much the medium is attenuating the incoming radiation and a large value of τ_0 retards the propagation of radiation within the medium requiring, as a consequence, a large time for reaching the steady-sate condition.

By taking the same system utilized in the prior simulation, the effects of the outer emissivities, ε_0 and ε_3, on the temperature distribution within the medium are analyzed. τ_0 is taken equal to unity. For the sake of symmetry, $\varepsilon_0 = \varepsilon_3$ and $\varepsilon_1 = \varepsilon_2$. The medium is a radiative dominant one, $NCR = 0.125$. Figure (4) shows the dimensionless transient temperature distribution in the medium until steady state is reached. It is observed that the temperature distribution is higher for the case in which $\varepsilon_0 = \varepsilon_3 = 0.25$ than for the case where all surfaces are black, especially for steady state condition.

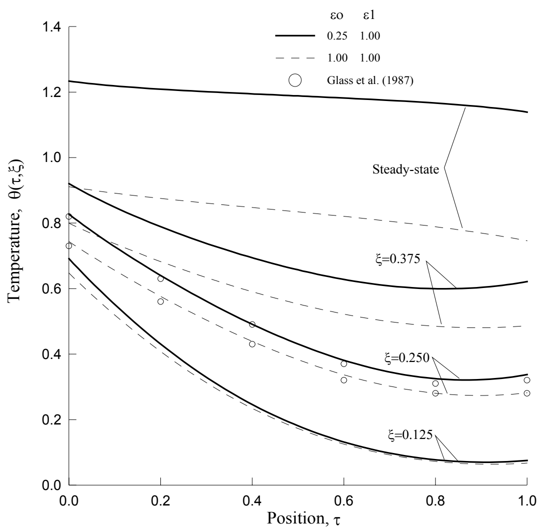

Figure 4: Effects of boundary surfaces emissivities on temperature distribution within the medium with NCR=0.125, $\tau_0 = 1.0$ and $\varepsilon_0 = \varepsilon_3$ and $\varepsilon_1 = \varepsilon_2$.

This phenomenon can be explained as follows: an outer and inner emissivities taken as unity implies that the surfaces are black, i.e., they absorb all energy that impinges on them. In this case, the amount of energy absorbed by the surface at $\tau = 0$ reaches its maximum value ($Q_{abs} = Q_0$), Eq. (2.a). Part of this absorbed energy will be emitted back to the exterior ambient by radiation and part will propagate to the inner regions of the medium by both conduction and radiation. When the outer emissivity is taken as 0.25, the surface at $\tau = 0$ will absorb a lower amount of energy as compared with the prior case. However, only a small part of the absorbed energy will be emitted back to the exterior ambient, because $\varepsilon_0 = 0.25$, the second term on Eq. (1.b), while the remaining energy will flow through the inner regions of the medium by both radiation and conduction. In other words, in spite of the absorbed energy be larger for the case in which the external surface is black, the total heat flux, i.e., radiation plus conduction, that propagates into the medium will be larger for the case in which the external surface has its emissivity equal to 0.25, leading to a higher level of temperature distribution within the medium. Numerical results obtained by Glass et al. (1987), by means of a composite Newton-Cotes integration method, are shown in the figure for $\xi = 0.250$.

Figure (4) also shows an increase in temperature during the transient near the surface at $\tau = 1.0$. To explain such a behavior, Fig. (5) shows the dimensionless radiation, conduction and total heat flux through the medium for the case in which $\varepsilon_0 = \varepsilon_3 = 0.25$. It can be observed that, for early times, the conduction heat flux becomes negative when $\tau \to \tau_0$, implying that, in these regions, $d\theta/d\tau > 0$. This phenomenon occurs because the surface at $\tau = 1.0$ is black, i.e., it absorbs all radiative energy that impinges on it. As a consequence, the surface temperature at $\tau = 1.0$ will rise faster than in the adjacent regions of the medium, where radiative absorption is smaller. This fact generates an inflection in the temperature distribution and, according to Fourier's law, a negative conduction heat transfer ($d\theta/d\tau > 0$). Figure (5) also shows the heat fluxes under steady state condition which, as expected, present a constant total heat flux along the medium. This behavior is in agreement with Fig. (4), which shows that the inflection in the temperature vanishes for steady state condition. For the sake of comparison, results obtained by Glass et al. (1987) are shown in the figure for $\xi = 0.250$.

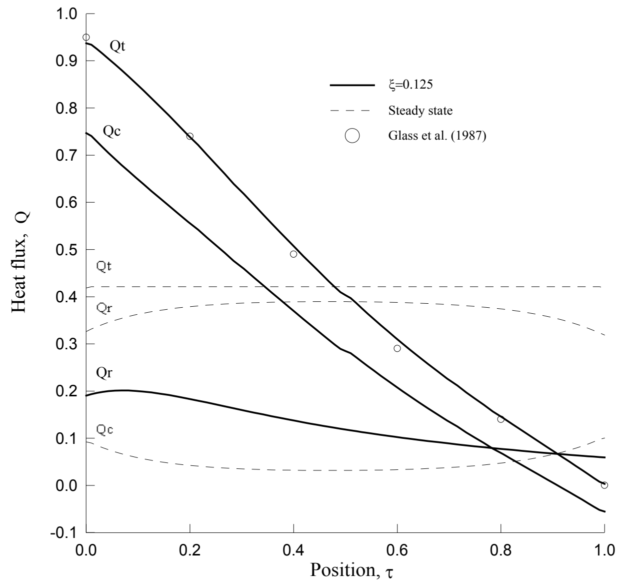

Figure 5: Conduction (Q^c), radiation (Q^r) and total (Q^t) dimensionless heat flux within the medium at time $\xi = 0.125$ and steady- state, with $NCR = 0.125$, $\tau_0 = 1$, $\varepsilon_0 = \varepsilon_3 = 0.25$ and $\varepsilon_1 = \varepsilon_2 = 1$.

We now consider a nonscattering medium formed by two layers of different materials. Each layer has the same optical thickness, $\tau_1 = \tau_2 = 5.0$. The outer emissivity of the surface at $\tau = 0$ is $\varepsilon_0 = 0.2$, whereas all other surfaces are assumed black. What differs one layer from another is the conduction-radiation parameter. While the layer on which is impinging the external heat flux is of conduction-dominant type, $NCR_1 = 2.5$, the other one is of radiation-dominant type, with $NCR_2 = 0.25$. Figure (6) illustrates the dimensionless transient temperature distribution in the medium until steady state is reached. The results obtained by Ho and Özisik (1987) for steady state condition are also shown in the figure.

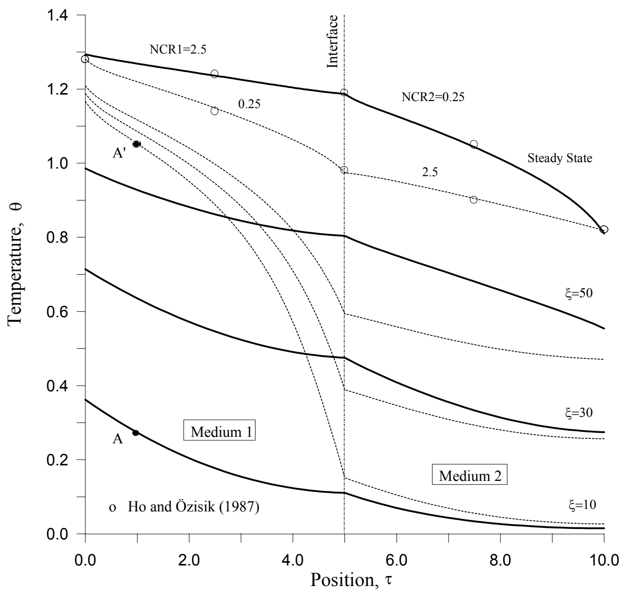

Figure 6: Effects of the conduction-radiation parameters on the transient and steady state temperature distribution for $\tau_1 = \tau_2 = 5.0$, $\omega_1 = \omega_2 = 0.0$, $\varepsilon_0 = 0.2$ and $\varepsilon_1 = \varepsilon_2 = \varepsilon_3 = 1.0$.

We can depict from Fig. (6) that when the medium is of radiation-dominant type, the slope of the temperature is larger than for a conduction-dominant medium. Under steady state condition, when the medium with NCR=0.25 is close to the hot surface ($\tau = 0$), the temperature distribution over the medium becomes lower than for the case in which the medium close to the hot surface has NCR=2.5. This difference in the slope of the temperature, for a given τ_0, is due to the attenuation of the radiative intensity as it propagates through the participant medium initially at zero temperature. This phenomenon is also observed for an optically thin medium (not shown in the figure), however, in this case the effect of NCR_1 and NCR_2 on the gradient temperature becomes less pronounced due to the fact that the resistance to radiation transfer decreases with decreasing optical thickness. Figure (6) also shows the transient behavior of the temperature distribution. As expected, where the medium is of radiation-dominant type, the temperature rises faster than for conduction-dominant medium, as shown by the points A and A' taken for a same τ and ξ. This difference in the temperature becomes less pronounced in the inner regions of the medium due to decay of the radiative intensity. It should be noted the strongly change in the temperature gradient at the interface. This fact can be explained observing Eq. (1.d). It is based on the energy conservation principle and means that the temperature gradient has to change in order to guarantee the continuity of the total heat flux at the interface. The CPU time spent in all simulations varied from about one minute until seven minutes by using a 350MHz Pentium II© Personal Computer.

5. Conclusions

The effects of the optical thickness, emissivities and conduction-radiation parameters on the transient and steady-state temperature distributions and heat flux within a medium composed by one and two layers of semitransparent materials were analyzed. The results showed that the conduction-radiation parameter can change significantly both the temperature distribution over the medium and the time necessary to reach steady state. These effects are related to the resistance to radiation transfer imposed by the medium. It has been shown that, as expected, the optical thickness can also affect the time necessary to reach steady state condition, besides to contribute to increase the medium's temperature as τ_0 increases. Finally, it was observed that, the larger the outer emissivities, ε_0 and ε_3, the lower the total heat flux that propagates into the medium, leading to a lower temperature distribution over the medium.

Concerning to the proposed method utilized to solve the radiative transfer equation, the obtained results are in very good agreement with those obtained by other authors.

6. References

Doornink, D.G. and Hering, R.G., 1972, "Transient Combined Conductive and Radiative Heat Transfer", Journal of Heat Transfer, pp. 473-478.

Genaro, G., Pessoa-Filho, J.B. and Rego, O.A.A., 2002, "Unsteady Combined Conduction-Radiation Heat Transfer in Multi-Layer Planar Participating Media", Proceedings of II National Congress of Mechanical Engineering, João Pessoa-PB, Brazil.

Genaro, G., Rego, O.A.A. and Pessoa-Filho, J.B., 2001, "One-Dimensional Combined Conduction-Radiation Heat Transfer in Multi-Layer Planar Participating Media", Proceedings of 16th Brazilian Congress of Mechanical Engineering, Vol. 4, pp. 497-506, Uberlândia-MG, Brazil.

Glass, D.E., Özisik, M.N. and McRae, D.S., 1987, "Combined Conduction and Radiation With Flux Boundary Condition for a Semi-Transparent Medium Covered by Thin Radiating Layers", J. of Quant. Spectrosc. Radiat. Transfer, Vol. 38, Nº 3, pp. 201-208.

Ho, C.-H. and Özisik, M.N., 1986, "Simultaneous Conduction and Radiation in a Two-Layer Planar Medium", J. Thermophysics, Vol. 1, Nº 2, pp. 154-159.

Ho, C.-H. and Özisik, M.N., 1987, "Combined Conduction and Radiation in a Two-Layer Planar Medium With Flux Boundary Condition", Numerical Heat Transfer, Vol. 11, pp. 321-340.

Modest, M.F., 1993, "Radiative Heat Transfer", McGraw-Hill, New York.

Özisik, M.N., 1973, "Radiative Transfer", Wiley, New York.

Pessoa-Filho, J.B. and Thynell, S.T., 1994, "Development of an Approximate Solution to the Equation of Transfer in Slab and Spherical Geometries", Journal of Quantitative Spectroscopy and Radiative Transfer, Vol. 52, No. 1, pp. 59-73.

Siegel, R., 1998, "Transient Effects of Radiative Transfer in Semitransparent Materials", International Journal of Engineering Science, pp. 1701-1739.

Tarshis, L. A., O'Hara, S. and Viskanta, R., 1969, "Heat Transfer by Simultaneous Conduction and Radiation for Two Absorbing Media in Intimate Contact", Int. J. of Heat and Mass Transfer, Vol. 12, pp. 333-347.

Viskanta, R., 1964, "Heat Transfer by Conduction and Radiation in Absorbing and Scattering Materials", Journal of Heat Transfer.

Weston, K.C. and Hauth, J.L., 1973, "Unsteady, Combined Radiation and Conduction in an Absorbing, Scattering and Emitting Medium", Journal of Heat Transfer, pp. 357-364.

Yuen, W.W. and Wong, L.W., 1980, "Heat Transfer by Conduction and Radiation in a One-Dimensional Absorbing, Emitting and Anisotropically-Scattering Medium", Journal of Heat Transfer, Vol. 102, pp. 303-307.